

Manuscript Number: CONBUILDMAT-D-14-01827R1

Title: Mechanical and hydration properties of ground granulated blastfurnace slag pastes activated with MgO-CaO mixtures

Article Type: Research Paper

Keywords: Alkali-activated slag; Reactive MgO; CaO; Hydration

Corresponding Author: Dr. Kai Gu, Ph.D.

Corresponding Author's Institution: Nanjing University

First Author: Kai Gu, Ph.D.

Order of Authors: Kai Gu, Ph.D.; Fei Jin, Ph.D.; Abir Al-Tabbaa, Ph.D.; Bin Shi, Ph.D.; Jin Liu, Ph.D.

Abstract: Since alkali-activated slag using conventional activators suffers from economical and technical problems, other alternative activators should be explored. This paper reports the results of an investigation into the activation of ground granulated blastfurnace slag by using 10% (by weight) reactive MgO, CaO and their mixtures with various ratios. The mechanical and hydration properties of pastes were examined up to 90 days. It was found that the strength of slag pastes activated with MgO-CaO mixtures decreased with the increasing ratio of MgO to CaO in the early age while a much steeper strength gain was observed in pastes with MgO/CaO higher than 19/1 after 28 days and longer. The addition of small amount of CaO in MgO can greatly accelerate the hydration of slag in the early age by increasing the pH of pore solution. However, pastes showed small difference in strength development at each period when MgO/CaO was less than 1. The main hydration products, analysed by XRD, TGA and SEM/EDS, were C-S-H and hydrotalcite-like phases. While CaO accelerated the formation of C-S-H in the early age, MgO induced more amount of hydrotalcite-like phases, which notably enhanced the strength of slag pastes with high MgO content after 28 days and longer. Calcite, portlandite and residual MgO were also observed, depending on the MgO/CaO ratio and the hydration time. This work indicated that the replacement of MgO by CaO can make the application of reactive MgO in slag activation more economical.

Mechanical and hydration properties of ground granulated blastfurnace slag pastes activated with MgO-CaO mixtures

Kai Gu^{1,2,*}, Fei Jin^{2,*}, Abir Al-Tabbaa², Bin Shi¹, Jin Liu³

¹ School of Earth Sciences and Engineering, Nanjing University, 163 Xianlin Avenue, Nanjing, China, 210093

² Department of Engineering, University of Cambridge, Trumpington Road, Cambridge, UK, CB2 1PZ

³ School of Earth Sciences and Engineering, Hohai University, 1 Xikang Road, Nanjing, China, 210098

*Corresponding authors: Kai Gu: gukainju@gmail.com, Fei Jin: fj232@cam.ac.uk

ABSTRACT: Since alkali-activated slag using conventional activators suffers from economical and technical problems, other alternative activators should be explored. This paper reports the results of an investigation into the activation of ground granulated blastfurnace slag by using 10% (by weight) reactive MgO, CaO and their mixtures with various ratios. The mechanical and hydration properties of pastes were examined up to 90 days. It was found that the strength of slag pastes activated with MgO-CaO mixtures decreased with the increasing ratio of MgO to CaO in the early age while a much steeper strength gain was observed in pastes with MgO/CaO higher than 19/1 after 28 days and longer. The addition of small amount of CaO in MgO can greatly accelerate the hydration of slag in the early age by increasing the pH of pore solution. However, pastes showed small difference in strength development at each period when MgO/CaO was less than 1. The main hydration products, analysed by XRD, TGA and SEM/EDS, were C-S-H and hydrotalcite-like phases. While CaO accelerated the formation of C-S-H in the early age, MgO induced more amount of hydrotalcite-like phases, which notably enhanced the strength of slag pastes with high MgO content after 28 days and longer. Calcite, portlandite and residual MgO were also observed, depending on the MgO/CaO ratio and the hydration time. This work indicated

1 that the replacement of MgO by CaO can make the application of reactive MgO in slag activation
2
3 more economical.
4
5
6

7
8 Keywords: Alkali-activated slag; Reactive MgO; CaO; Hydration
9
10
11
12
13
14
15
16
17
18
19
20
21
22
23
24
25
26
27
28
29
30
31
32
33
34
35
36
37
38
39
40
41
42
43
44
45
46
47
48
49
50
51
52
53
54
55
56
57
58
59
60
61
62
63
64
65

1. Introduction

Climate change, attributed by large to greenhouse gas emissions, has been a major threat to human society. Among the most energy-intensive industries, the cement industry contributes ~5-8% of global man-made CO₂ emissions [1], mainly because of the direct calcination of limestone and the consumption of fossil fuels. The search for more sustainable binders has led to the development of alkali-activated cements (AACs), which utilise a large portion of supplementary cementitious materials (SCMs), such as blastfurnace slag, fly ash, metakaolin and silica fume [2,3].

The most widely used activators in AAC are sodium silicate, sodium hydroxide, sodium carbonate or a mixture of sodium-potassium hydroxide with sodium silicate-potassium silicate [1,4]. However, most of these activators do not exist naturally and they are obtained from energy intensive manufacturing processes, which expands the energy consumption associated with AAC.

A comparison of the carbon dioxide equivalent (CO₂-e) emissions between alkali-activated fly ash and ordinary PC indicated that only ~9% reduction was obtained by using the former instead of ~26-80% (as previously claimed [5,6]) when considering the energy consumption associated with the manufacturing process of activators [7]. Other issues should also be carefully considered when using these conventional activators, including the fast setting time, the high drying shrinkage, the highly corrosive nature of alkali solutions, the viscosity of alkali solution and the heat released by the dissolution of the alkali compounds, especially alkali hydroxide, during preparation of the solutions [1,8–10]. In order to tackle the above mentioned technical and environmental challenges associated with the conventional alkali activators used in AAC, alternative sustainable and cost effective activators should be explored.

1 Regarding to ground granulated blastfurnace slag (GGBS), calcium hydroxide [Ca(OH)₂] and
2
3 calcium oxide (CaO) have been reported to be potential activators because they are easily obtained
4
5 and are much less expensive than sodium hydroxide or sodium silicate [9,11]. Slag concrete
6
7 activated with Ca(OH)₂, with different auxiliary activators (Na₂SO₄ and Na₂CO₃), performed
8
9 enhanced workability, delayed setting time and a similar increasing rate of compressive strength to
10
11 PC concrete [12]. The comparison between the effect of CaO and Ca(OH)₂ in activating slag
12
13 revealed that the use of CaO demonstrated a superior potential for the activation of GGBS and
14
15 produced a higher mechanical strength than Ca(OH)₂ [11].
16
17
18
19
20
21

22 More recently, studies have indicated that reactive magnesia (MgO) could also serve as an
23
24 effective activator for GGBS, showing its advantages in mechanical performances and the
25
26 controllable setting time (which depends on the reactivity of MgO) [13–18]. The results by Yi et
27
28 al. [17] showed that the reactive MgO activated GGBS achieved higher 28-day compressive
29
30 strength than that of the corresponding Ca(OH)₂-GGBS system due to the larger content of the
31
32 voluminous hydrotalcite-like phases having formed during the hydration. A later study proved that
33
34 although reactive MgO-GGBS blends showed a lower slag hydration degree, they had better pore
35
36 filling effect which resulted in higher 90-day strengths than the corresponding Ca(OH)₂-GGBS
37
38 blends [18]. However, the early age strength of reactive MgO-GGBS blends was also found to be
39
40 too low when the MgO content was <10-15wt% [18]. Although enhanced early strengths were
41
42 observed by using MgO of higher reactivity [16], the cost becomes a concern. The current global
43
44 production of MgO is ~20 million tonnes per year (~80% of which is produced in China, mainly
45
46 from magnesite mines and the rest is produced from brines and seawater) [18] and the price of
47
48 MgO with potential in slag activation varies from US\$180 per ton to US\$350 per ton in China
49
50
51
52
53
54
55
56
57
58
59
60
61
62
63
64
65

1 [19], which is lower than, for instance, NaOH (~US\$500 per ton in China). Nevertheless, the cost
2
3 of MgO usage needs further reduction. The study on the effect of different MgOs on the activation
4
5 efficiency of GGBS by Jin et al. [16] showed that the reactive MgO containing the highest content
6
7 of internal CaO produced higher UCS values, which was attributed to their higher pH of the pore
8
9 solution and higher slag hydration degrees compared to those relatively purer MgOs. In this
10
11 context, the mixture of MgO-CaO is worthy of investigating as a economically and technically
12
13 feasible activator for GGBS because CaO is cheap (~US\$70 per ton in China) . As a natural
14
15 mixture of MgO-CaO, calcined dolomite has already been reported to be an effective activator to
16
17
18
19
20
21
22
23
24
25
26
27
28
29
30
31
32
33
34
35
36
37
38
39
40
41
42
43
44
45
46
47
48
49
50
51
52
53
54
55
56
57
58
59
60
61
62
63
64
65

In the present study, seven MgO-CaO mixtures were used to activate slag in order to explore the influence of MgO/CaO ratio on the mechanical and hydration properties of slag pastes. The strength and the hydration degree of slag were examined by the unconfined compressive strength (UCS), pH of pore water and a selective dissolution method. The hydration products and the microstructural characteristics of MgO-CaO activated GGBS were thoroughly studied by thermogravimetric analysis (TGA), X-ray diffraction (XRD) and scanning electron microscope (SEM) imaging combined with energy-dispersive X-ray (EDX) analysis. Meanwhile, the influence of water to binder ratio (0.35, 0.38) and curing conditions of the paste samples (water cured and humidity cured) were also presented.

2. Materials and experimental procedures

2.1. Materials

The commercial materials used in this research included reactive MgO (grade 92/200 from Richard Baker Harrison, UK), CaO (from Tarmac and Buxton Lime and Cement, UK), and GGBS

1 (from Hanson, UK). The chemical compositions and physical properties for these materials are
2
3 given in Table 1. The reactivity of the reactive MgO is ~100 s determined by the acetic acid test
4
5 according to Shand [21] and is categorised as a medium reactive MgO [18].
6
7

8 9 *2.2. Sample preparation*

10
11 In the blends, the total amount of the activator (including MgO and/or CaO) was kept
12
13 constant at 10% by weight. Seven mix formulations, as shown in Table 2, were prepared by
14
15 changing the proportion of MgO and CaO, at water to binder ratios of 0.35 and 0.38. The
16
17 nomenclature used for the samples was a combination referring to the contents of MgO and CaO
18
19 in the mixes. For instance, M2.5C7.5 refers to the samples of 2.5% MgO and 7.5% CaO. Materials
20
21 were fully mixed in dry form and then a pre-determined amount of water was added. After
22
23 homogeneously mixed in a mixer, samples were casted into 40mm×40mm×40mm cubes covered
24
25 with cling film and cured at 20°C. After 24h, samples were demoulded and cured under two
26
27 different conditions: (1) immersed in deionised water and (2) sealed in plastic boxes at relative
28
29 humidity of 99±1%. For both conditions, the curing temperature was kept constant at 20±1°C.
30
31
32
33
34
35
36
37
38
39

40 *2.3. Experimental procedures*

41
42 UCS measurements, using a constant load rate of 2400 N/sec, were undertaken in triplicate
43
44 paste samples after curing for 7, 28 and 90 days. After the compression tests, the fractured paste
45
46 samples were ground below 425 µm and then 10 g sample was weighted to mix with deionised
47
48 water at a liquid to solid ratio of 1 ml/g in airtight containers according to [22]. The readings were
49
50 taken in duplicate after 24 hours using a pH meter (Eutech 520) with an accuracy of ±0.01.
51
52 Hydration of fractured paste samples were arrested by immersion in excess acetone for 3 days
53
54 followed by vacuum dried for at least 3 days and oven dried for 1 day at 35°C. After drying, the
55
56
57
58
59
60
61
62
63
64
65

1 fractured pastes were gold coated for SEM/EDS analysis and also finely ground below 75 μm for
2
3 XRD, TGA and selective dissolution tests. SEM/EDS were performed on JEOL 5800 and
4
5
6 approximately 10 points on the gel were picked for the determination of elemental composition.
7
8
9 Siemens D5000 X-ray diffractometer was used to collect XRD data with a scanning range
10
11 between 5° and $55^\circ 2\theta$. The scanning speed of 1 s/step and resolution of 0.05° /step were applied.
12
13
14 Samples for TGA were heated from 40°C to 1000°C in air with the rate of heating at $10^\circ\text{C}/\text{min}$ on
15
16
17 a Perkin Elmer STA 6000 machine. The hydration degree of slag was determined by a selective
18
19
20 dissolution method using salicylic acid/methanol/acetone in duplicate according to Luke and
21
22
23 Glasser [23]. This method is preferable to ethylene diamine tetraacetic acid
24
25 (EDTA)/triethanolamine/NaOH technique due to the formation of hydrotalcite-like phase
26
27
28 [11,15,24].
29
30

31 **3. Results and discussions**

32 *3.1. Strength development*

33
34
35
36
37
38 The strength development of the pastes with varying MgO/CaO ratios is shown in Fig.1 for
39
40
41 the two different curing conditions and the specified w/c ratios. Generally, the strength of samples
42
43
44 cured under the high humidity conditions was observed to be smaller than those of the water cured
45
46
47 samples regardless of the curing age.

48
49 After 7 days, water cured samples with 10% CaO content (M0C10) gained strength of
50
51
52 $\sim 25\text{MPa}$. The maximum strength was achieved when the MgO/CaO ratio was 1 (M5C5) and then
53
54
55 it decreased significantly by the increase of the MgO content. It should be noted that the M10C0
56
57
58 paste only gained $\sim 8\text{MPa}$ strength after 7 days, but a small amount of CaO addition (M9.5C0.5)
59
60
61 resulted in a remarkable strength increase ($\sim 16\text{MPa}$). The strength development after 28 days was
62
63
64
65

1 similar to that at 7 days for pastes with $\leq 8.5\%$ MgO while the strength for pastes with $\geq 9.5\%$
2
3 MgO (M9.5C0.5 and M10C0) increased more sharply, achieving $\sim 25\text{MPa}$. Compared with that at
4
5
6 7 days, the difference between M9.5C0.5 and M10C0 pastes was much smaller, especially for
7
8
9 samples under high humidity curing, showing approximately the same strength. After 90 days, the
10
11 strength of pastes M9.5C0.5 and M10C0 increased more notably to 41.8MPa and 42.6MPa ,
12
13 respectively, while the strength gained by other samples were relatively moderate. It was found
14
15 that the strength for paste M10C0 was $\sim 10\%$ higher than that of M0C10 after 90 days, which is
16
17 consistent with [18], who observed that reactive MgO outperformed lime in the long-term when
18
19 activating GGBS.
20
21
22
23

24
25 For the samples prepared with w/c of 0.38 (Fig.1b), the compressive strength was, on average,
26
27 $\sim 27.4\%$, $\sim 16.8\%$ and $\sim 17.4\%$, respectively, smaller than the pastes with w/c of 0.35 after each age,
28
29 but with a similar trend to the pastes with w/c of 0.35. It was found that the water to binder ratio
30
31 showed greater influence on the strengths in the early age.
32
33
34
35

36 For both w/c ratios, it can be seen that a small CaO content ($\sim 0.5\%$) significantly increased
37
38 the early strength of high MgO-containing samples while it did not have much of an effect on the
39
40 long term strength (90 days) of the pastes (Fig.1). On the other hand, the strength of all the pastes
41
42 which contained $\leq 5\%$ MgO showed inconspicuous difference at different times.
43
44
45
46

47 *3.2. pH evolution*

48
49

50 Various research indicates that pH has a significant effect on the hydration process of
51
52 activated slag systems and also the nature of the products generated [25–34]. Higher pH
53
54 environments usually induce better slag activation and higher mechanical strength. In order to
55
56
57
58
59
60
61
62
63
64
65

1 effectively activate the hydration of slag, the pH should be ≥ 11.5 [30,31]. It was also reported that,
2
3 on the other hand, pH values < 12 would delay the activation process [35].
4
5

6 Fig.2 presents the pH variations of the pastes with w/c of 0.35. All pH values except for paste
7
8 M10C0 at 7 days were observed to be ≥ 12 . For paste M10C0, the relatively low pH, compared to
9
10 other CaO containing pastes, resulted in a slow hydration process and hence much lower strength,
11
12 especially at 7 days. By contrast, pastes containing CaO presented much higher pH between 12.0
13
14 and 12.3 in the early age. At 28 days, pH of pastes containing CaO increased to ~ 12.5 due to the
15
16 equilibrium of Ca(OH)_2 in pore solution while that of paste M10C0 was still at a low level. At 90
17
18 days, the pH of the pastes with $\geq 1.5\%$ CaO content maintained pH of ~ 12.5 due to the sufficient
19
20 presence of CaO providing sufficient OH^- after hydration and the equilibrium between the
21
22 hydration products and the pore solution still existing. By contrast, those with less CaO decreased
23
24 to ~ 12.3 which was induced by the consumption of Ca(OH)_2 through the reaction with GGBS. The
25
26 pH of paste M10C0 continued to increase at 90 days, indicating the latent hydration of MgO and
27
28 the hysteretic releasing of OH^- into the pore water. It should be noted that, compared with paste
29
30 M10C0, a small dosage of CaO in the blend (i.e. paste M9.5C0.5) was associated with greatly
31
32 increased pH at 7 and 28 days. Therefore the hydration was significantly accelerated in such high
33
34 MgO content pastes during these periods.
35
36
37
38
39
40
41
42
43
44
45
46

47 *3.3. Hydration kinetics*

48 *3.3.1. Slag dissolution*

49
50
51
52
53 The percentage of anhydrous slag after different hydration periods allows the calculation of
54
55 the fraction of slag reacted. Fig.3 presents the degrees of reacted slag of the water cured pastes
56
57 with water to binder ratio of 0.35. An increase of MgO (and simultaneously a decrease of CaO)
58
59
60
61
62
63
64
65

1 content in the blends is observed to decrease the hydration degree (Fig.3) except for pastes
2
3 M9.5C0.5 and M10C0 after 90 days, whose degree of hydration were observed to be boosted.
4
5
6 Although the degree of reacted slag of pastes M10C0 and M9.5C0.5 were still lower than the other
7
8 pastes, except for paste M8.5C1.5, they showed higher strengths than others which could be
9
10 explained by the nature of the hydration products (as discussed later in Section 3.4). When the
11
12 MgO/CaO ratio was ≤ 1 , the samples showed only a moderate degree of hydration gain reaching
13
14 values between 26.0% and 28.4% after 90 days, indicating that the hydration reaction was very
15
16 fast during the early age but slowed down at later ages. The hydration process of paste M10C0
17
18 was very slow during the first 7 days (at 9.3%), but revealed high values ~21.0% after 90 days.
19
20 Obviously, the presence of a little CaO induced a higher degree of reacted slag of paste M9.5C0.5
21
22 than M10C0 at each corresponding time.
23
24
25
26
27
28
29
30

31 *3.3.2. Chemically bound water content*

32
33 The chemically bound water content obtained by measuring the weight loss up to 650°C
34
35 using TGA could be used as a measure of the hydration kinetics of blended cements [36–38]. To
36
37 eliminate the influence of decomposition of calcite, weight loss up to 550°C was measured here
38
39 although this may underestimate the amount of chemically bound water from slag hydration than
40
41 was really happening since some portlandite may be consumed by carbonation during curing. The
42
43 weight loss after 550°C was mainly attributed to the decomposition of calcite. Nevertheless,
44
45 according to the weight losses given in Fig.4, the hydration gradually slowed down with the
46
47 increasing content of MgO in the paste in the early age. After 28 days and longer, however, the
48
49 water loss of different pastes showed smaller differences. For those with MgO content higher than
50
51
52
53
54
55
56
57
58
59
60
61
62
63
64
65

1 9.5%, sharp increases in weight loss were observed with hydration time and the bound water
2
3 content were not necessarily smaller than others pastes after 28 days and longer.
4
5

6 The development trend in bound water content were slightly different from that in the degree
7
8 of reacted slag (Fig.3). For instance, although the degree of reacted slag of M10C0 after 90 days
9
10 was smaller than M0C10, their bound water contents were very close. It was attributed to the
11
12 higher amount of hydrotalcite-like phases (discussed below) increased the bound water content of
13
14 high MgO content pastes as the hydrotalcite-like phases ($\text{Mg}_4\text{Al}_2\text{O}_7 \cdot 10\text{H}_2\text{O}$) contains relatively
15
16 more water than C-S-H [39].
17
18
19
20
21
22
23

24 3.4. Hydrates

25 3.4.1. X-ray diffraction

26
27 Fig.5 presents the X-ray diffraction patterns of pastes hydrated for 28 days in water. As the
28
29 main hydration products of alkali-activated slag, C-S-H and hydrotalcite-like phases, can be
30
31 clearly identified in all pastes agreeing with the literature [11,31,34,37,40]. Due to their
32
33 semi-amorphous nature, the major peaks of C-S-H appeared with the background hump in the 2θ
34
35 range of 25° to 35° . Hydrotalcite-like phases are common hydration products in alkali-activated
36
37 GGBS when there is sufficient MgO content in the GGBS composition [41–44], hence it is not
38
39 surprising to observe hydrotalcite-like phases in GGBS pastes activated by reactive MgO
40
41 associated with CaO.
42
43
44
45
46
47
48
49
50
51

52 In high CaO content pastes (i.e. M0C10 and M5C5), the strong peaks corresponding to
53
54 portlandite are detected, which can be attributed to the excess CaO added. On the other hand, the
55
56 peaks of portlandite were not detected in the microgram of M9.5C0.5 and M10C0 (samples with
57
58
59
60
61
62
63
64
65

1 low content of CaO) due to its complete consumption in forming C-S-H and hydrotalcite-like
2
3 phases after 28 days. The presence of calcite in M0C10 and M5C5 could have originated from the
4
5 raw CaO and/or the carbonation of the formed portlandite. Unhydrated MgO phase observed
6
7 around $43^{\circ}2\theta$ indicates the surplus supply of MgO for activating the slag in pastes M9.5C0.5 and
8
9 M10C0. MgO present in cementitious system is predicted to precipitate initially as brucite [45].
10
11 However, brucite was not detected here, in agreement with the previous studies [17,18]. It may
12
13 have converted to hydrotalcite-like phases although the formation of brucite was not confirmed
14
15 when the XRD test performed.
16
17
18
19
20
21
22

23 3.4.2. Thermogravimetric analysis (TGA) 24 25 26

27 The TG/DTG curves of samples after 28 days hydration are given in Fig.6. At up to 300°C ,
28
29 the weight loss mainly corresponding to the thermal decomposition of C-S-H, according to
30
31 [11,17,34,38,46], were observed in all pastes. The small shoulders around 80°C present the
32
33 decomposition of ettringite [47,48], which originates from the sulphate content in the raw GGBS
34
35 and CaO. However, this minor hydration product was not identified in the XRD result, probably
36
37 due to its small content. The decomposition of the hydrotalcite-like phases induced a tiny shoulder
38
39 at $\sim 200^{\circ}\text{C}$ and the weight loss between 330°C and 400°C , as reported by other researchers
40
41 [38,48,49]. For pastes of high CaO content (i.e. M0C10 and M5C5), the dehydroxylation of
42
43 portlandite can be observed at $\sim 440^{\circ}\text{C}$. Beyond 600°C , considerable amount of $-\text{CO}_3^{2-}$ containing
44
45 phases (mainly calcite) are observed, agreeing well with the XRD result.
46
47
48
49
50
51
52
53

54 To quantitatively analyse the amounts of the two hydration products (i.e. C-S-H and
55
56 portlandite) after different hydration time, the weight losses between 40°C to 300°C and 400°C and
57
58 500°C can be calculated separately. Here define the weight loss of C-S-H in the former range as
59
60
61
62
63
64
65

1 Δm_1 and that of portlandite between 400°C and 500°C as Δm_2 . Although the decomposition of
2
3 other phases (ettringite, hydrotalcite-like phases) overlaps with C-S-H within this range, their
4
5 influence is supposed to be small due to their relatively small amounts. In addition, the
6
7 decomposition temperature of hydrotalcite-like phases overlaps with that of portlandite, therefore
8
9 Δm_2 was over estimated to some extent especially for pastes with high MgO content. The
10
11 variations of Δm_1 and Δm_2 of samples over hydration time are summarised in Fig.7. Fig.7a
12
13 reveals that the weight loss of C-S-H accounted for approximately 4.9% of the ignited weight in
14
15 paste M0C10 and it gradually dropped to ~2.6% of that in paste M10C0 in the early age. It can be
16
17 explained by the increased hydration rate which was in positive correlation with the content of
18
19 CaO. Δm_1 increased with the curing time due to the increased hydration degree as suggested by
20
21 Fig.3 and the increments of paste M9.5C0.5 and M10C0 were relatively greater. After 28 days, the
22
23 weight loss of these two pastes were close to, although still smaller, other samples (CaO wt.% \geq
24
25 2.5%) but almost at the same level by 90 days.
26
27

28
29
30
31
32
33
34
35
36 In general, Δm_2 showed a negative relationship with MgO content and a positive relationship
37
38 with time (Fig.7b). It is not surprising because the hydration of CaO produces portlandite therefore
39
40 more CaO resulted in more portlandite. On the other hand, since no apparent characteristic peaks
41
42 of portlandite were detected in XRD curves of M9.5C0.5 and M10C0 (Fig.5), Δm_2 of these two
43
44 samples after 28 days and 90 days can be attributed to the decomposition of hydrotalcite-like
45
46 phases whose weight loss also appears around 400°C [17,34,38]. In this context, it can be
47
48 concluded that more hydrotalcite-like phases formed in pastes with MgO content higher than 9.5%
49
50 after 28 days and longer, therefore made significant contribution to the strength by its better pore
51
52 filling effect.
53
54
55
56
57
58
59
60
61
62
63
64
65

3.4.3. Scanning electron microscopy

Fig.8 shows the SEM images of microstructure of selected paste samples after 28 days hydration. Dense C-S-H gels can be observed in all samples. The formation of plates of portlandite in Fig.8a and apparent presence of platelet hydrotalcite-like phases in Fig.8b and c agree well with the analyses by XRD and TGA (Fig.5 and Fig.6).

Fig.9b shows a much denser M9.5C0.5 microstructure of 90 days that that of 28 days (Fig.9a) in a different scale bar. It may be attributed to (i) more C-S-H formed after longer hydration according to Fig.7a and (ii) the significantly pore filling effect hydrotalcite-like phases, which are more voluminous than C-S-H. That more hydrotalcite-like phases formed in pastes in high MgO content was confirmed by TG analysis (see Section 3.4.2).

3.4.4. Energy-dispersive X-ray microanalysis

Combined with SEM, EDS analysis was conducted to determine the differences in the elemental composition of the hydrate phases. The Ca/Si and Mg/Al ratios calculated from chemical compositions of the anhydrous binders (see Table 1) are summarised in Table 3. These initial ratios varied due to the different dosages of added MgO and CaO. The average ratios obtained from EDS analysis are also given in Table 3.

For alkali-activated slag, previous research suggested that the Ca/Si ratio of C-S-H gel ranges from 0.6 to 2.3, depending on the type of activator, the curing condition and the nature of the slag [30,34,42,43,50]. Table 3 shows that after 28 days, the Ca/Si ratio of the gel decreased from 1.59 for M0C10 to 1.45 for M10C0, in agreement with the initial Ca/Si ratio, which decreased from 1.46 to 1.16 when the CaO content decreased from 10% to 0%. Pastes with a higher pH (>11.5)

1 pore solution were reported to have a lower Ca/Si ratio due to the fact that the solubility of Si
2
3 increased with pH while that of Ca decreased [30,31]; the slight increase of Ca/Si ratio with the
4
5 increase of CaO content is attributed to the increased Ca^{2+} ion availability and hence higher uptake
6
7 of Ca^{2+} ion in C-S-H gel.
8
9

10
11 The Mg/Si versus Al/Si ratios are plotted in Fig.10 for all hydration periods together. The
12
13 linear slope confirms the presence of hydrotalcite-like phases with Mg/Al ratio from 1.32 for paste
14
15 M0C10 to 1.93 for paste M10C0, which are higher than the initial Mg/Al ratios given in Table 3.
16
17 Increasing the MgO content resulted in a higher Mg/Al ratio of the hydration products due to the
18
19 increased availability of Mg ions for reaction. In addition, the intercept bigger than 0.2 in the Al/Si
20
21 axis suggests that the C-S-H gel contains significant proportions of aluminium, agreeing well with
22
23 others [18,24].
24
25
26
27
28
29
30

31 **4. Conclusions**

32
33
34
35 Ground granulated blastfurnace slag was activated using reactive MgO, CaO, and MgO-CaO
36
37 mixtures and their mechanical and hydration properties were studied. Based on the experimental
38
39 results, the following conclusions can be drawn:
40
41

42
43 (1) The performance of slag pastes activated with MgO-CaO mixtures depended on the ratio
44
45 of MgO to CaO. The strength of slag pastes decreased with the increasing ratio of MgO to CaO in
46
47 the early age while a much steeper strength gain was observed in pastes with MgO to CaO ratio
48
49 higher than 19/1 (i.e. M9.5C0.5 and M10C0) after 28 days and longer. Pastes showed small
50
51 difference in strength development at each period when the ratio of MgO to CaO was less than 1.
52
53
54

55 (2) The addition of CaO in MgO can increase the pH of the pore solution, and hence
56
57 significantly accelerate the activation of slag in the early age. In this study, 0.5% CaO blended
58
59
60
61

1 with 9.5% MgO was found to notably increase the early strength of the paste.
2

3 (3) The hydration degree of slag decreased with the increasing MgO/CaO ratio, but this
4 trend was not applicable for pastes with MgO/CaO ratios higher than 19/1 after 90 days due to the
5 delayed activation of the slag by MgO.
6
7
8

9 (4) XRD and TGA results showed that the hydration products of activated slag using
10 MgO-CaO mixtures were mainly C-S-H and hydrotalcite-like phases. Portlandite and calcite were
11 also observed and their quantities depended on the MgO/CaO ratio. The amount of C-S-H was
12 found to be in positive correlation to the content of CaO in slag in the early age while more
13 hydrotalcite-like phases formed in high MgO content pastes after 28 days and longer.
14
15
16
17
18
19
20
21
22
23

24 (5) By increasing the MgO/CaO ratio in the mixture, the average Ca/Si ratio of C-S-H gels
25 after 28 days decreased from 1.59 to 1.45. The Mg/Al ratio for the hydrotalcite-like phases varied
26 from 1.3 to 1.9, depending on the MgO/CaO ratio.
27
28
29
30
31
32

33 (6) For MgO-CaO-GGBS system, higher compressive strengths of pastes can be achieved
34 by lower w/c ratio and using water curing instead of humidity curing.
35
36
37
38
39

40 **Acknowledgements**

41 The work presented in this paper was carried out at Department of Engineering, University of
42 Cambridge, where the first author was a visiting researcher. The visit was funded by the China
43 Scholarship Council and the Scientific Research Foundation of the Graduate School of Nanjing
44 University (No.2012CL11). The financial support for the PhD studentship of the second author
45 from the Cambridge Trust and China Scholarship Council was also very much appreciated.
46
47
48
49
50
51
52
53
54
55
56
57

58 **References**

- 1
2
3
4
5
6
7
8
9
10
11
12
13
14
15
16
17
18
19
20
21
22
23
24
25
26
27
28
29
30
31
32
33
34
35
36
37
38
39
40
41
42
43
44
45
46
47
48
49
50
51
52
53
54
55
56
57
58
59
60
61
62
63
64
65
- [1] Provis JL, van Deventer JSJ. Alkali Activated Materials: State-of-the-Art Report, RILEM TC 224-AAM. Dordrecht: Springer Netherlands; 2014.
 - [2] Shi C, Jiménez AF, Palomo A. New cements for the 21st century: The pursuit of an alternative to Portland cement. *Cem Concr Res* 2011;41:750–63.
 - [3] Provis JL. Geopolymers and other alkali activated materials: why, how, and what? *Mater Struct* 2013;47:11–25.
 - [4] Rashad AM. A comprehensive overview about the influence of different additives on the properties of alkali-activated slag – A guide for Civil Engineer. *Constr Build Mater* 2013;47:29–55.
 - [5] Habert G, d’Espinose de Lacaillerie JB, Roussel N. An environmental evaluation of geopolymer based concrete production: reviewing current research trends. *J Clean Prod* 2011;19:1229–38.
 - [6] Duxson P, Provis JL, Lukey GC, van Deventer JSJ. The role of inorganic polymer technology in the development of “green concrete.” *Cem Concr Res* 2007;37:1590–7.
 - [7] Turner LK, Collins FG. Carbon dioxide equivalent (CO₂-e) emissions: A comparison between geopolymer and OPC cement concrete. *Constr Build Mater* 2013;43:125–30.
 - [8] Yang K-H, Song J-K, Ashour AF, Lee E-T. Properties of cementless mortars activated by sodium silicate. *Constr Build Mater* 2008;22:1981–9.
 - [9] Yang K-H, Cho A-R, Song J-K, Nam S-H. Hydration products and strength development of calcium hydroxide-based alkali-activated slag mortars. *Constr Build Mater* 2012;29:410–9.
 - [10] Van Deventer JSJ, Provis JL, Duxson P. Technical and commercial progress in the adoption of geopolymer cement. *Miner Eng* 2012;29:89–104.
 - [11] Kim MS, Jun Y, Lee C, Oh JE. Use of CaO as an activator for producing a price-competitive non-cement structural binder using ground granulated blast furnace slag. *Cem Concr Res* 2013;54:208–14.
 - [12] Yang K-H, Cho A-R, Song J-K. Effect of water–binder ratio on the mechanical properties of calcium hydroxide-based alkali-activated slag concrete. *Constr Build Mater* 2012;29:504–11.
 - [13] Shen W, Wang Y, Zhang T, Zhou M, Li J, Cui X. Magnesia modification of alkali-activated slag fly ash cement. *J Wuhan Univ Technol Sci Ed* 2011;26:121–5.
 - [14] Li X. Mechanical properties and durability performance of reactive magnesium cement concrete, PhD thesis. University of Cambridge, UK, 2012.

- 1
2
3
4
5
6
7
8
9
10
11
12
13
14
15
16
17
18
19
20
21
22
23
24
25
26
27
28
29
30
31
32
33
34
35
36
37
38
39
40
41
42
43
44
45
46
47
48
49
50
51
52
53
54
55
56
57
58
59
60
61
62
63
64
65
- [15] Jin F, Abdollahzadeh A, Al-Tabbaa A. Effect of different MgO on the hydration of MgO-activated granulated ground blastfurnace slag paste. Proc. Int. Conf. Sustain. Constr. Mater. Technol., Kyoto, Japan: 2013.
- [16] Jin F, Gu K, Abdollahzadeh A, Al-Tabbaa A. Effect of different reactive MgOs on the hydration of MgO-activated ground granulated blastfurnace slag paste. J Mater Civ Eng 2014;doi:10.1061/(ASCE)MT.1943-5533.0001009.
- [17] Yi Y, Liska M, Al-Tabbaa A. Properties and microstructure of GGBS–magnesia pastes. Adv Cem Res 2013:1–9.
- [18] Jin F. Characterisation and Performance of reactive MgO-based cements, PhD thesis. University of Cambridge, UK, 2014.
- [19] Beijing HL Consulting Company. Market research report on magnesia(MgO)industry in China 2009. 2009.
- [20] Gu K, Jin F, Al-Tabbaa A, Shi B. Activation of ground granulated blast furnace slag by using calcined dolomite. Constr Build Mater 2014;doi:10.1016/j.conbuildmat.2014.06.044.
- [21] Shand MA. The chemistry and technology of magnesia. Hoboken, New Jersey: John Wiley & Sons; 2006.
- [22] Hidalgo A, Garcia JL, Aloson MC, Fernandez-Luco L, Andrade C. Testing methodology for pH determination of cementitious materials. application to low pH binders for use in HLNWR. In: Bäckblom G, editor. 2nd Work. R&D low-pH Cem. a Geol. Repos., Madrid: 2005.
- [23] Luke K, Glasser F. Selective dissolution of hydrated blast furnace slag cements. Cem Concr Res 1987;17:273–82.
- [24] Ben Haha M, Lothenbach B, Le Saout G, Winnefeld F. Influence of slag chemistry on the hydration of alkali-activated blast-furnace slag — Part II: Effect of Al₂O₃. Cem Concr Res 2012;42:74–83.
- [25] Roy A, Schilling PJ, Eaton HC, Malone PG, Brabston WN, Wakeley LD. Activation of Ground Blast-Furnace Slag by Alkali-Metal and Alkaline-Earth Hydroxides. J Am Ceram Soc 1992;75:3233–40.
- [26] Wang S, Scrivener K, Pratt P. Factors affecting the strength of alkali-activated slag. Cem Concr Res 1994;24:1033–43.
- [27] Wang S-D, Scrivener KL. Hydration products of alkali activated slag cement. Cem Concr Res 1995;25:561–71.

- 1
2
3
4
5
6
7
8
9
10
11
12
13
14
15
16
17
18
19
20
21
22
23
24
25
26
27
28
29
30
31
32
33
34
35
36
37
38
39
40
41
42
43
44
45
46
47
48
49
50
51
52
53
54
55
56
57
58
59
60
61
62
63
64
65
- [28] Shi C, Day R. Some factors affecting early hydration of alkali-slag cements. *Cem Concr Res* 1996;26:439–41.
- [29] Bakharev T, Sanjayan JG, Cheng Y-B. Alkali activation of Australian slag cements. *Cem Concr Res* 1999;29:113–20.
- [30] Song S, Jennings H. Pore solution chemistry of alkali-activated ground granulated blast-furnace slag. *Cem Concr Res* 1999;29:159–70.
- [31] Song S, Sohn D, Jennings H, Mason T. Hydration of alkali-activated ground granulated blast furnace slag. *J Mater Sci* 2000;35:249–57.
- [32] Li Y, Sun Y. Preliminary study on combined-alkali–slag paste materials. *Cem Concr Res* 2000;30:963–6.
- [33] Oh JE, Monteiro PJM, Jun SS, Choi S, Clark SM. The evolution of strength and crystalline phases for alkali-activated ground blast furnace slag and fly ash-based geopolymers. *Cem Concr Res* 2010;40:189–96.
- [34] Ben Haha M, Le Saout G, Winnefeld F, Lothenbach B. Influence of activator type on hydration kinetics, hydrate assemblage and microstructural development of alkali activated blast-furnace slags. *Cem Concr Res* 2011;41:301–10.
- [35] Fernández-Jiménez A, Puertas F. Effect of activator mix on the hydration and strength behaviour of alkali-activated slag cements. *Adv Cem Res* 2003;15:129–36.
- [36] Bhatti J. A review of the application of thermal analysis to cement-admixture systems. *Thermochim Acta* 1991;189:313–50.
- [37] Escalante-García JI, Fuentes AF, Gorokhovskiy A, Fraire-Luna PE, Mendoza-Suarez G. Hydration Products and Reactivity of Blast-Furnace Slag Activated by Various Alkalis. *J Am Ceram Soc* 2003;86:2148–53.
- [38] Gruskovnjak A, Lothenbach B, Winnefeld F, Münch B, Figi R, Ko S-C, et al. Quantification of hydration phases in supersulfated cements: review and new approaches. *Adv Cem Res* 2011;23:265–75.
- [39] Ben Haha M, Lothenbach B, Le Saout G, Winnefeld F. Influence of slag chemistry on the hydration of alkali-activated blast-furnace slag — Part I: Effect of MgO. *Cem Concr Res* 2011;41:955–63.
- [40] Puertas F, Martínez-Ramírez S. Alkali-activated fly ash/slag cements: strength behaviour and hydration products. *Cem Concr Res* 2000;30:1625–32.

- 1
2
3
4
5
6
7
8
9
10
11
12
13
14
15
16
17
18
19
20
21
22
23
24
25
26
27
28
29
30
31
32
33
34
35
36
37
38
39
40
41
42
43
44
45
46
47
48
49
50
51
52
53
54
55
56
57
58
59
60
61
62
63
64
65
- [41] Brough AR, Atkinson A. Sodium silicate-based , alkali-activated slag mortars Part I . Strength , hydration and microstructure 2002;32:865–79.
- [42] Richardson J, Biernacki J. Stoichiometry of slag hydration with calcium hydroxide. *J Am Ceram Soc* 2002;85:947–53.
- [43] Richardson I, Brough A, Groves G, Dobson C. The characterization of hardened alkali-activated blast-furnace slag pastes and the nature of the calcium silicate hydrate (CSH) phase. *Cem Concr Res* 1994;24:813–29.
- [44] Le Saoût G, Ben Haha M, Winnefeld F, Lothenbach B. Hydration Degree of Alkali-Activated Slags: A ^{29}Si NMR Study. *J Am Ceram Soc* 2011;94:4541–7.
- [45] Lothenbach B, Winnefeld F. Thermodynamic modelling of the hydration of Portland cement. *Cem Concr Res* 2006;36:209–26.
- [46] Michel M, Georgin J-F, Ambroise J, Péra J. The influence of gypsum ratio on the mechanical performance of slag cement accelerated by calcium sulfoaluminate cement. *Constr Build Mater* 2011;25:1298–304.
- [47] Lothenbach B, Wieland E. A thermodynamic approach to the hydration of sulphate-resisting Portland cement. *Waste Manag* 2006;26:706–19.
- [48] Gruskovnjak A, Lothenbach B, Winnefeld F, Figi R, Ko S-C, Adler M, et al. Hydration mechanisms of super sulphated slag cement. *Cem Concr Res* 2008;38:983–92.
- [49] Parashar P, Sharma V, Agarwal DD, Richhariya N. Rapid synthesis of hydrotalcite with high antacid activity. *Mater Lett* 2012;74:93–5.
- [50] Wang S-D, Scrivener KL. ^{29}Si and ^{27}Al NMR study of alkali-activated slag. *Cem Concr Res* 2003;33:769–74.

The list of captions for all tables:

1. **Table 1. Chemical compositions and physical properties of raw materials (from suppliers' datasheets)**
2. **Table 2. Mix compositions of the pastes**
3. **Table 3. Atomic ratios obtained by theoretical calculation and EDS analyses**

1
2
3
4
5
6
7
8
9
10
11
12
13
14
15
16
17
18
19
20
21
22
23
24
25
26
27
28
29
30
31
32
33
34
35
36
37
38
39
40
41
42
43
44
45
46
47
48
49
50
51
52
53
54
55
56
57
58
59
60
61
62
63
64
65

The list of captions for all figures:

- 1
- 2
- 3 **1. Fig.1 Compressive strength of the pastes at two different water/binder ratios of (a) $w/c=0.35$ and (b)**
- 4 **$w/c=0.38$.**
- 5
- 6
- 7 **2. Fig.2 pH variation of water cured pastes with time, $w/c=0.35$.**
- 8
- 9 **3. Fig.3 Variation of degree of reacted slag with MgO content, $w/c=0.35$.**
- 10
- 11 **4. Fig.4 Weight loss between 40°C and 550°C determined by TGA (weight percentage relative to the**
- 12 **ignited samples), $w/c=0.35$.**
- 13
- 14
- 15 **5. Fig.5 XRD patterns of selected samples after 28 days.**
- 16
- 17 **6. Fig.6 TG/DTG curves of samples after a hydration time of 28 days.**
- 18
- 19 **7. Fig.7 Weight losses in two temperature ranges (a) Δm_1 and (b) Δm_2 .**
- 20
- 21 **8. Fig.8 Representative SEM images of hydrated samples after 28 days showing the typical hydration**
- 22 **products: A: C-S-H, B: portlandite, C: hydrotalcite-like phases for three different pastes at 28 days: (a)**
- 23 **M0C10, (b) M9.5C0.5 and (c) M10C0.**
- 24
- 25
- 26
- 27 **9. Fig.9 SEM images of C0.5M9.5 after two different hydration periods. (a) 28 days, (b) 90 days.**
- 28
- 29
- 30 **10. Fig.10 Atomic ratios Mg/Si vs. Al/Si of the samples after 28 days.**
- 31
- 32
- 33
- 34
- 35
- 36
- 37
- 38
- 39
- 40
- 41
- 42
- 43
- 44
- 45
- 46
- 47
- 48
- 49
- 50
- 51
- 52
- 53
- 54
- 55
- 56
- 57
- 58
- 59
- 60
- 61
- 62
- 63
- 64
- 65

Table 1[Click here to download Table: Table 1.docx](#)**Table 1. Chemical compositions and physical properties of raw materials (from suppliers' datasheets)**

	GGBS	MgO	CaO
Chemical composition			
SiO ₂	37.0	0.9	0.9
Al ₂ O ₃	13.0	0.22	0.13
CaO	40.0	0.9	94.0
MgO	8.0	>93.2	0.5
K ₂ O	0.6	-	-
Na ₂ O	0.3	-	-
SO ₃	1.0	-	0.06
Fe ₂ O ₃	-	0.5	0.08
CaCO ₃	-	-	3.7
Physical properties			
Specific surface area(m ² /g)	0.49	9.00	-
Bulk density (kg/m ³)	1050	-	1020

Table 2[Click here to download Table: Table 2.docx](#)**Table 2. Mix compositions of the pastes**

Sample	activator/ slag	MgO/ CaO	weight percentage(%)			water/binder
			MgO	CaO	GGBS	
M0C10		0/10	0	10	90	0.35 & 0.38
M2.5C7.5		1/3	2.5	7.5	90	0.35
M5C5		1/1	5	5	90	0.35 & 0.38
M7.5C2.5	1/9	3/1	7.5	2.5	90	0.35
M8.5C1.5		17/3	8.5	1.5	90	0.35 & 0.38
M9.5C0.5		19/1	9.5	0.5	90	0.35 & 0.38
M10C0		10/0	10	0	90	0.35 & 0.38

Table 3[Click here to download Table: Table 3.docx](#)**Table 3. Atomic ratios obtained by theoretical calculation and EDS analyses**

Sample	Age (days)	Ca/Si	Mg/Al
M0C10	initial	1.46	0.79
	28	1.59	-
M5C5	initial	1.31	1.29
	28	1.56	-
	90	1.54	-
M9.5C0.5	initial	1.17	1.75
	7	1.12	-
	28	1.57	-
	90	2.07	-
M10C0	initial	1.16	1.80
	28	1.45	-

Figure 1
[Click here to download high resolution image](#)

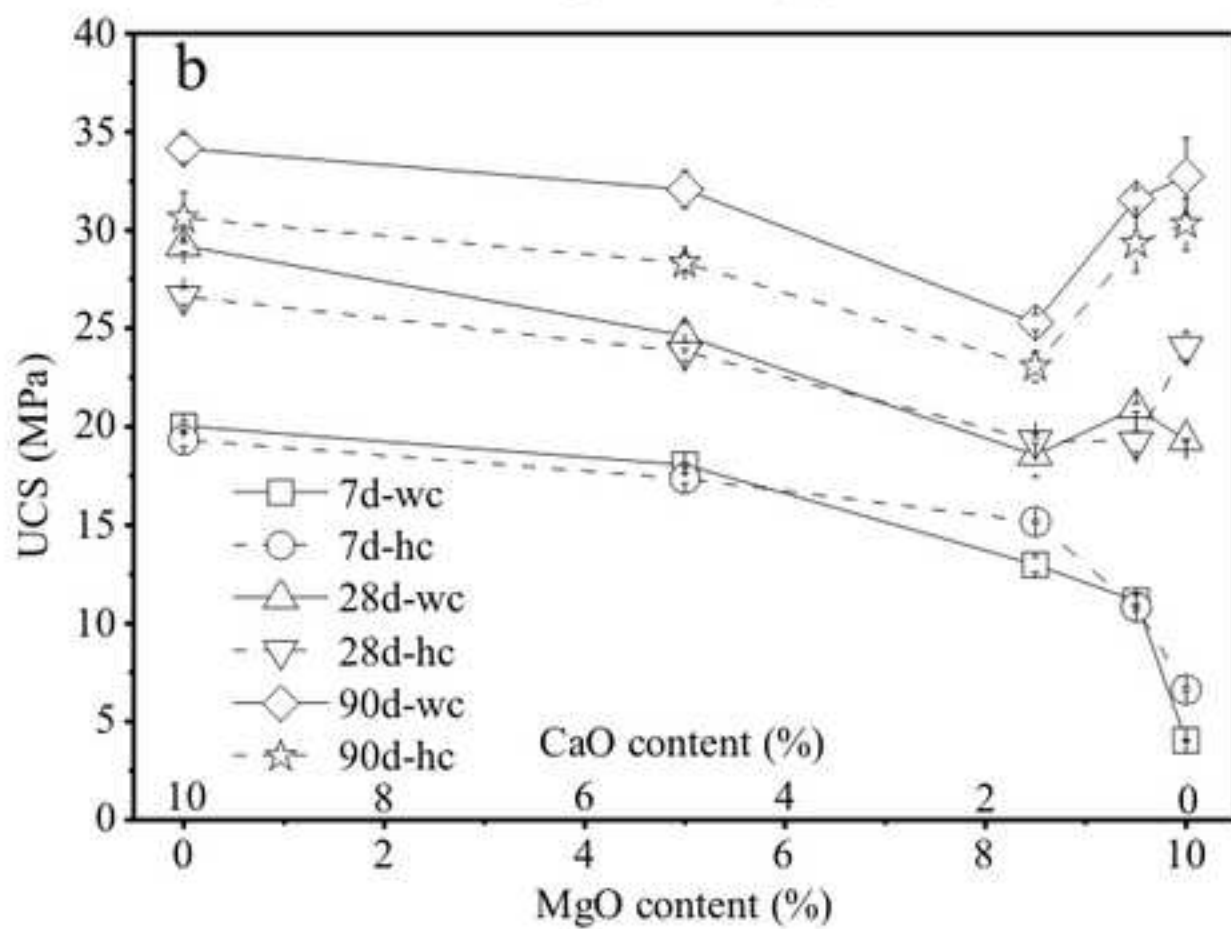
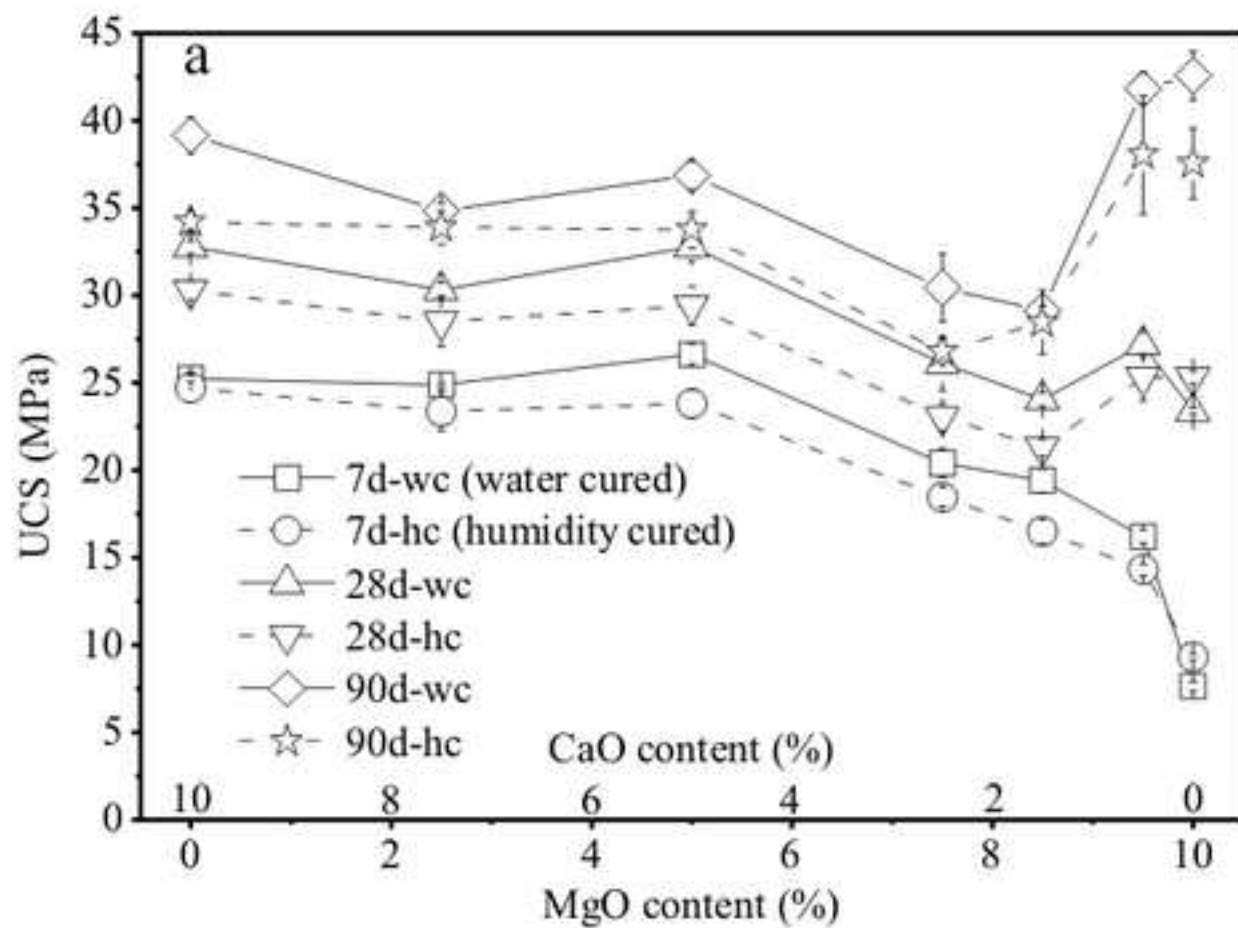


Figure 2
[Click here to download high resolution image](#)

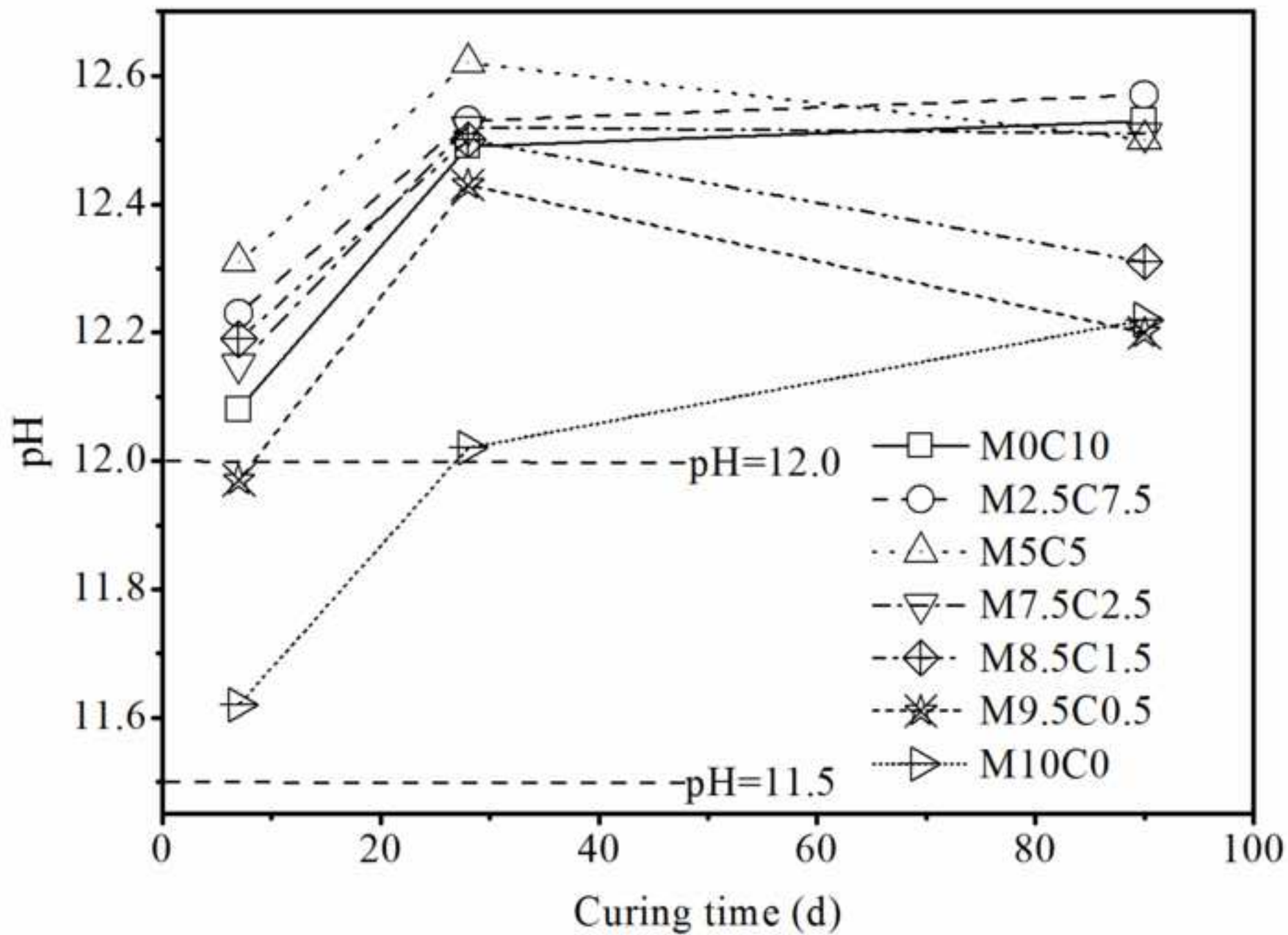


Figure 3
[Click here to download high resolution image](#)

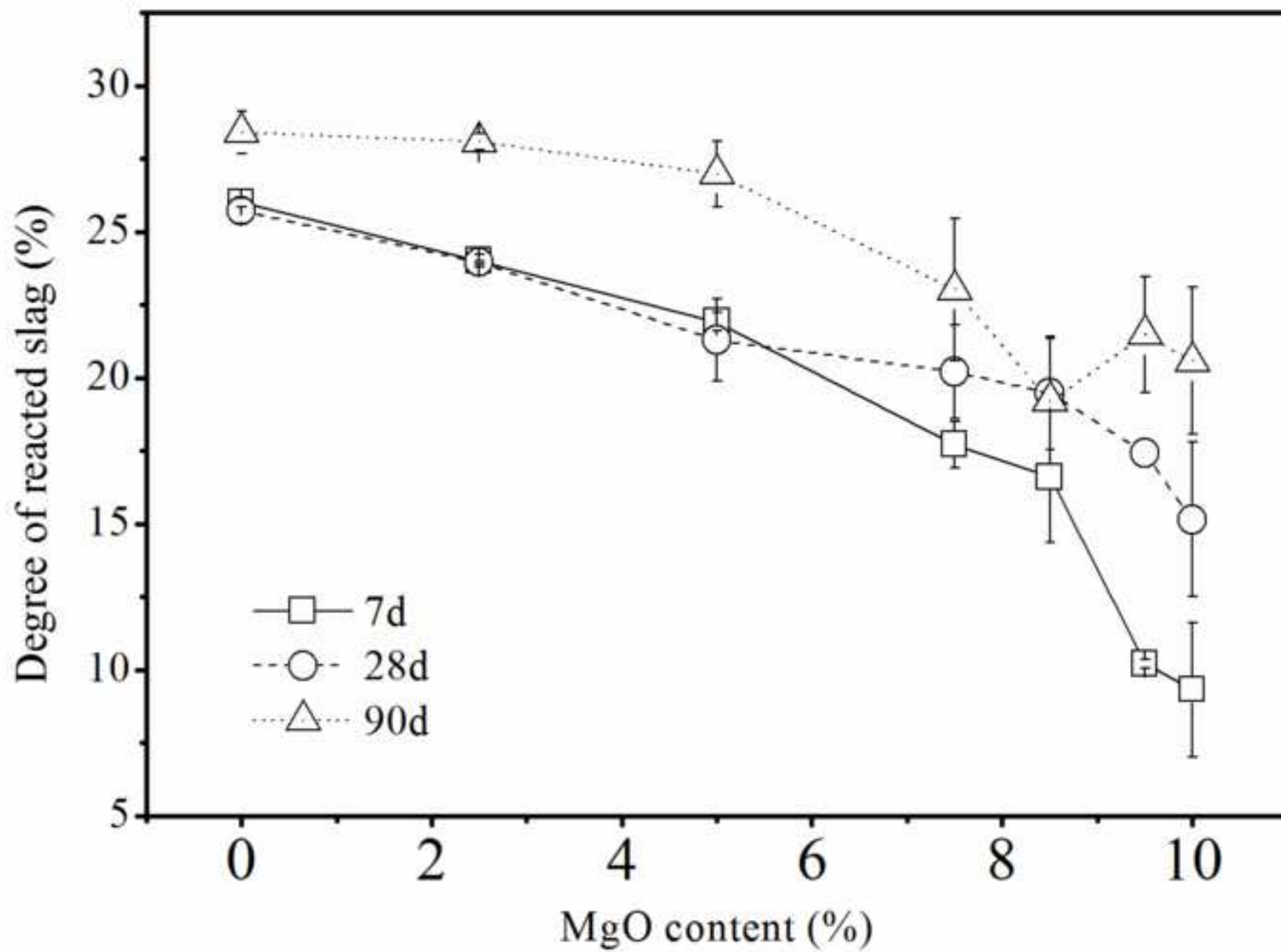


Figure 4
[Click here to download high resolution image](#)

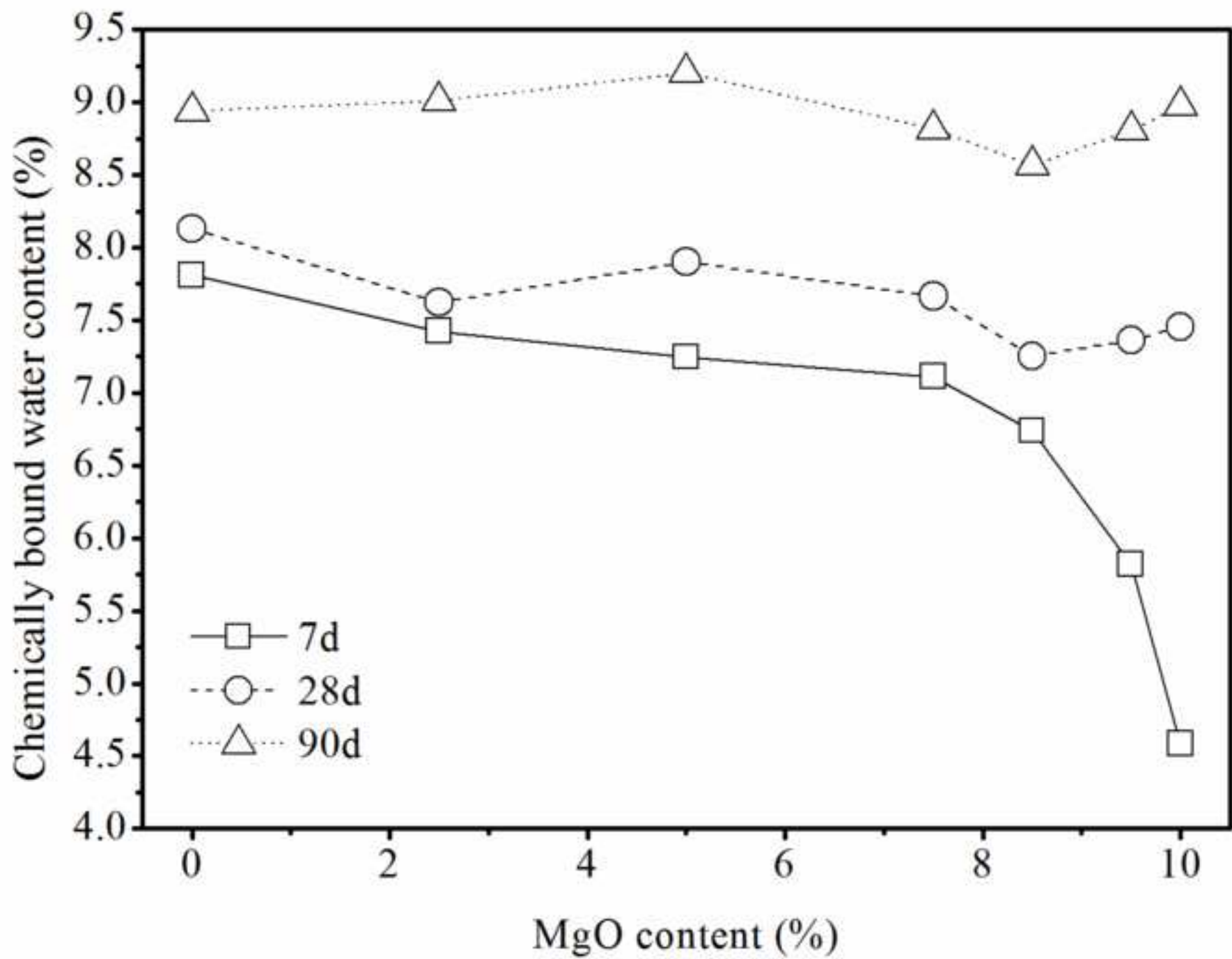


Figure 5

[Click here to download high resolution image](#)

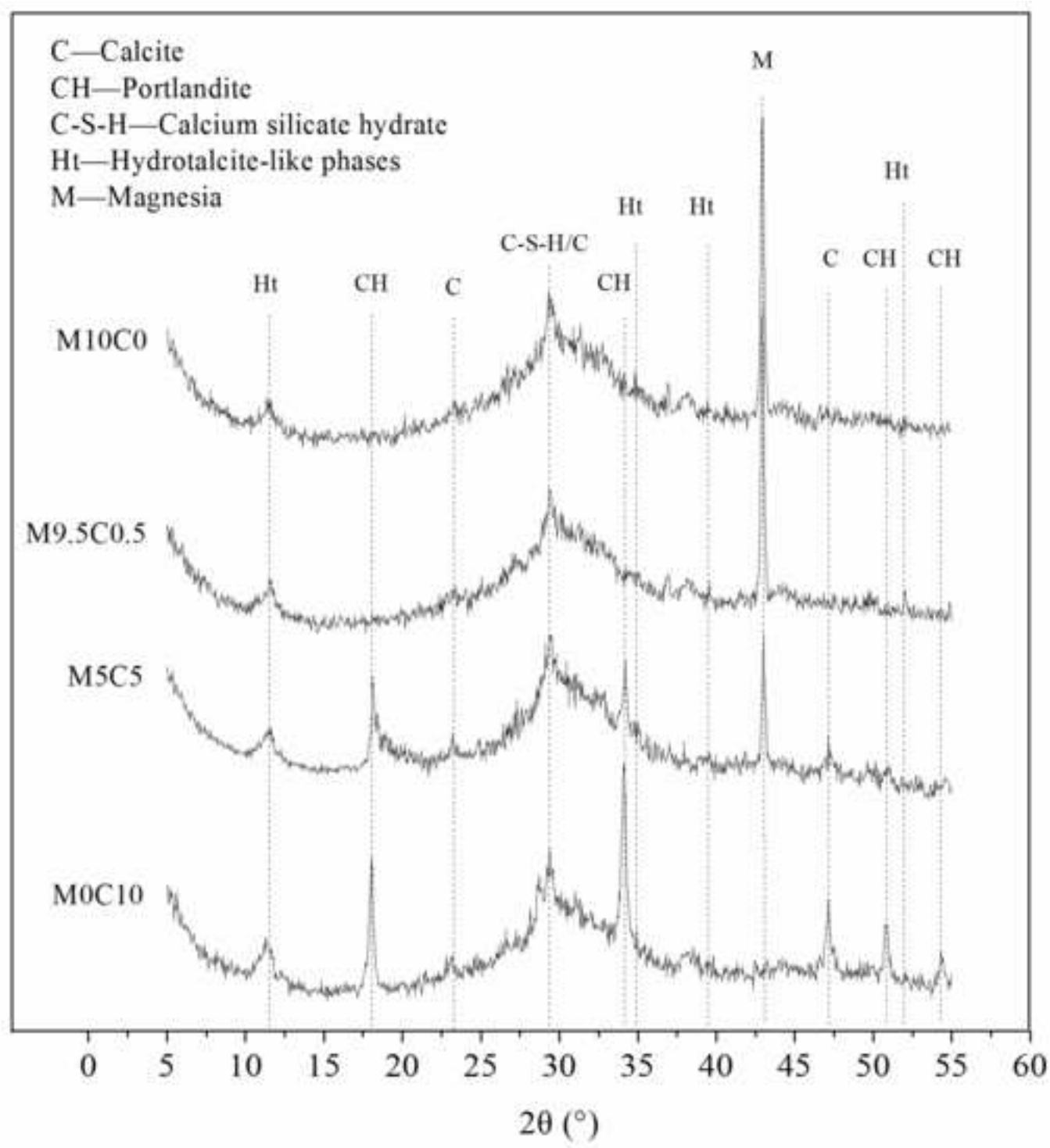


Figure 6
[Click here to download high resolution image](#)

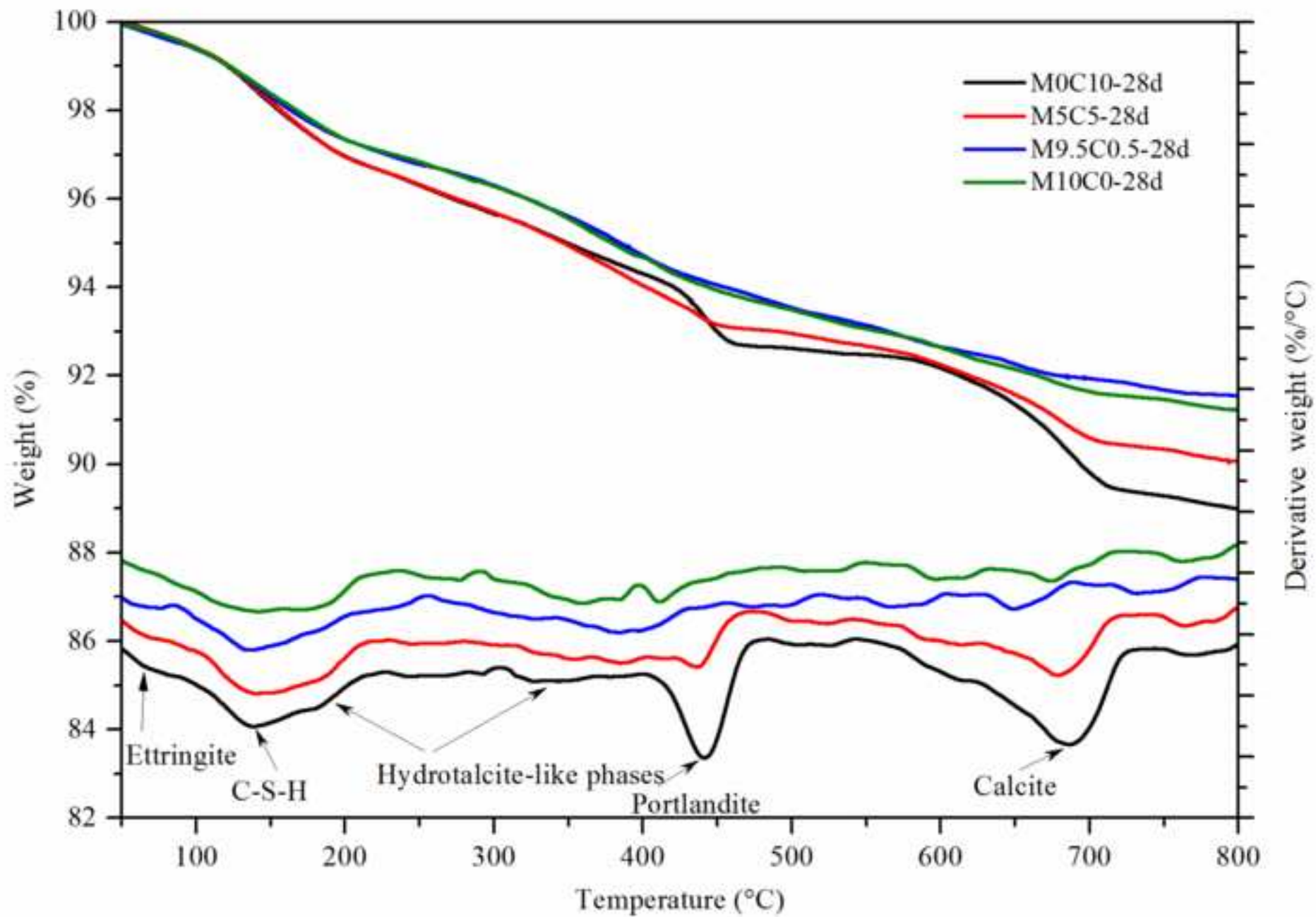


Figure 7
[Click here to download high resolution image](#)

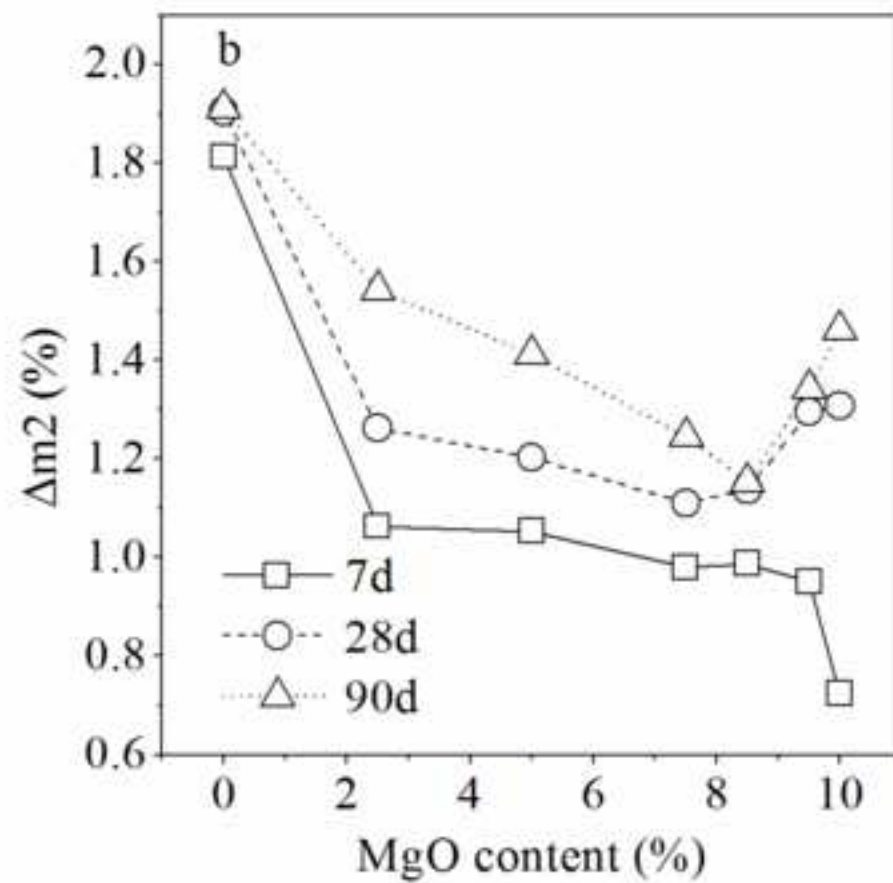
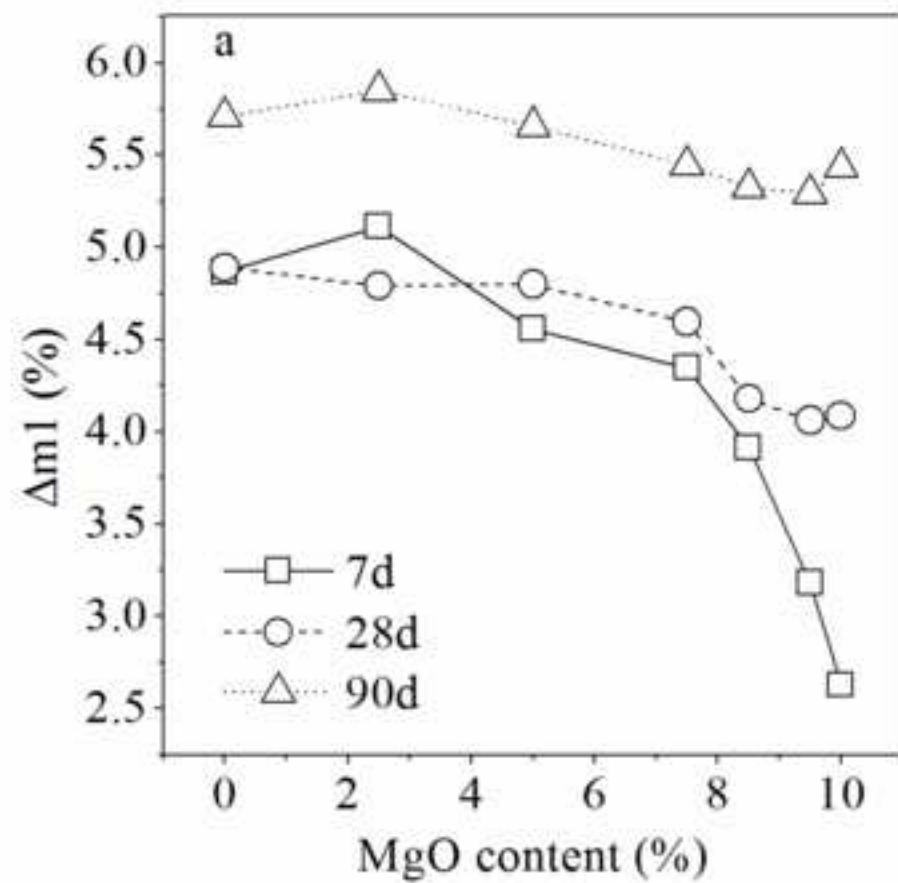
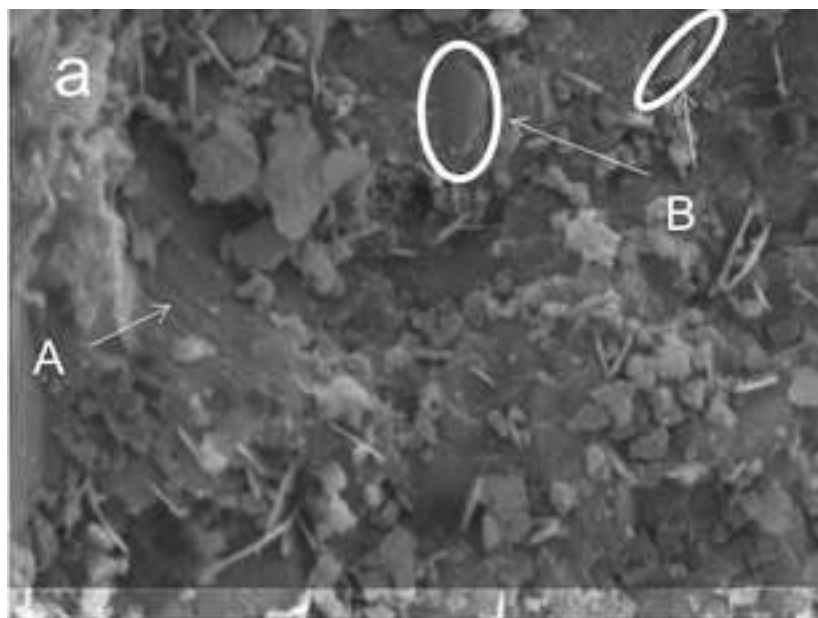
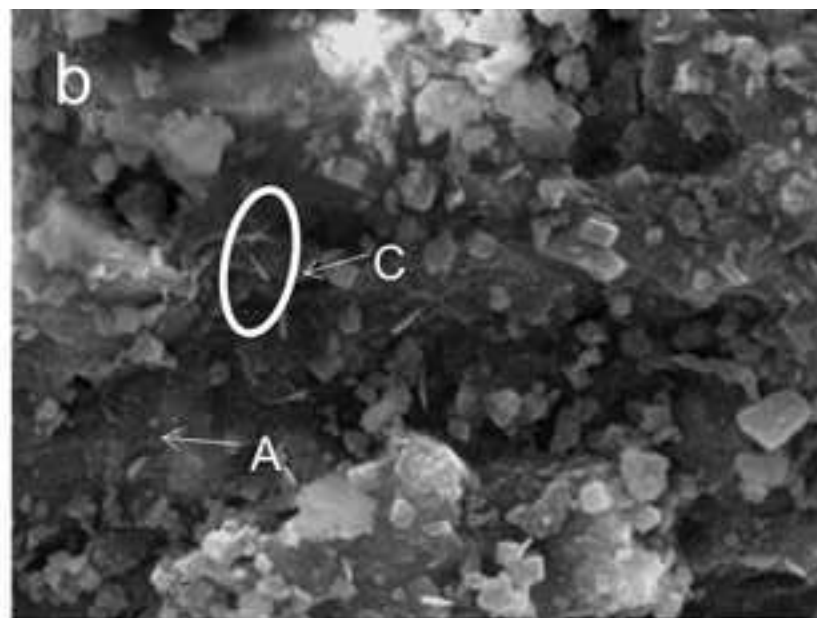


Figure 8
[Click here to download high resolution image](#)



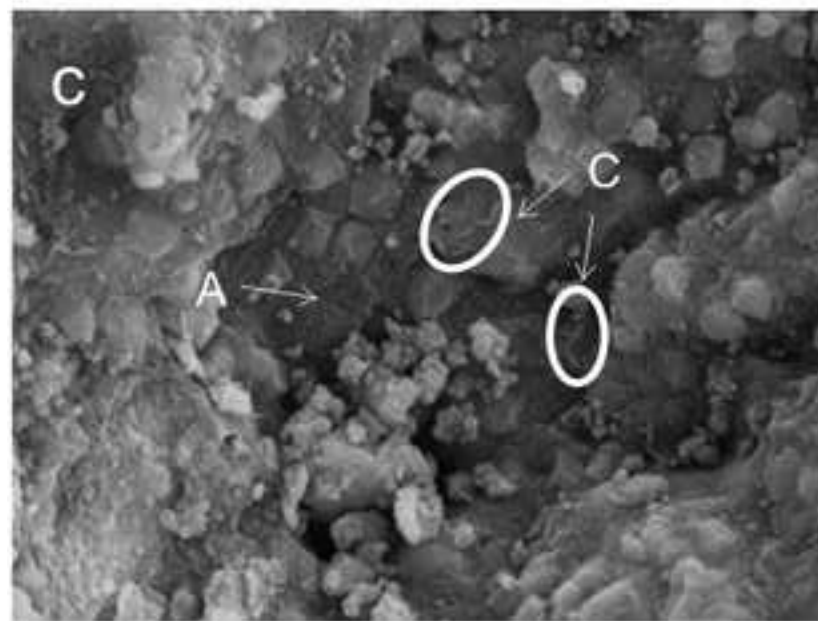
10µm

M0C10-28d



10µm

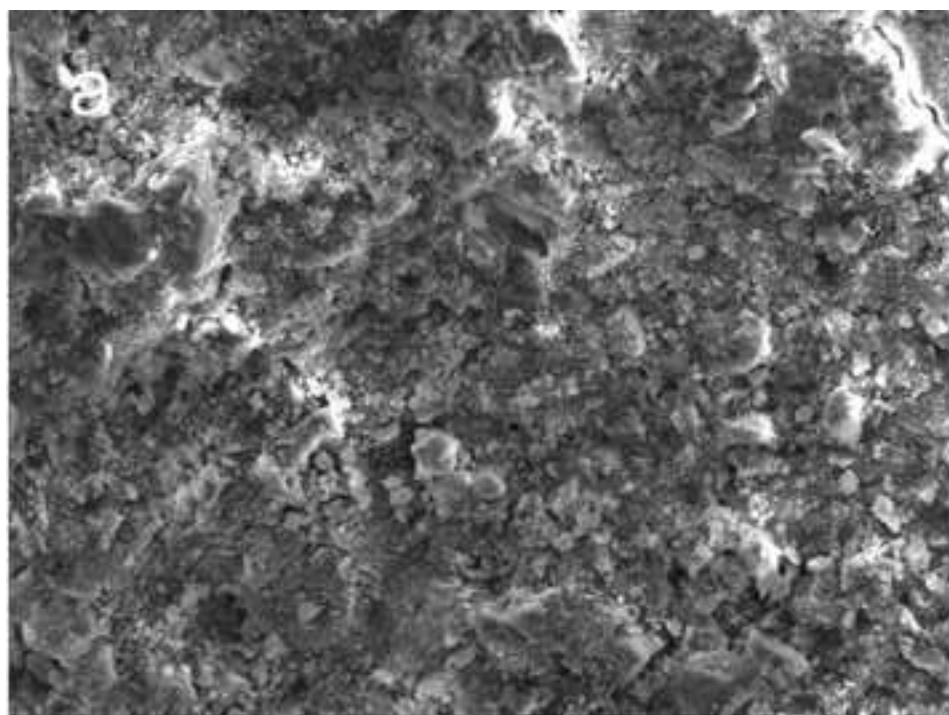
M9.5C0.5-28d



10µm

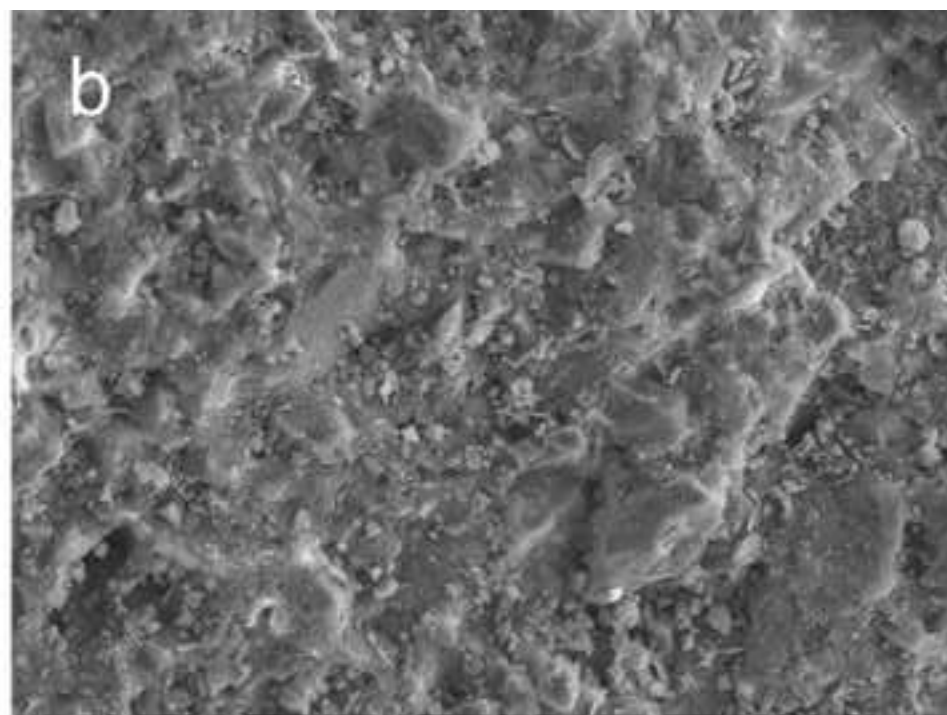
M10C0-28d

Figure 9
[Click here to download high resolution image](#)



100 μ m

M9.5C0.5-28d



100 μ m

M9.5C0.5-90d

Figure 10
[Click here to download high resolution image](#)

